

Piotr NIESLONY<sup>1</sup>  
Wit GRZESIK<sup>1</sup>  
Piotr LASKOWSKI<sup>2</sup>  
Krzysztof ZAK<sup>1</sup>

## **NUMERICAL 3D FEM SIMULATION AND EXPERIMENTAL ANALYSIS OF TRIBOLOGICAL ASPECTS IN TURNING INCONEL 718 ALLOY**

This paper presents 3D FEM simulation results performed for the power law and JC (Johnson-Cook) material constitutive models for two sets of friction parameters. The friction conditions were tested using pin-on-disc tribometer. Machining tests were carried out using carbide cutting tools coated with a TiAlN monolayer without coolants. The selection of machining conditions was based on real production data. In addition, a real CAD model of the cutting tool insert was implemented. Moreover, an advanced technique of meshing the cutting edge and the grooved rake face was applied. The simulations include cutting forces and cutting temperature. Finally, FEM simulations were compared with measurements in order to improve the simulation strategy.

### **1. INTRODUCTION**

The machining of difficult-to-machine materials such as heat resistant superalloys is still currently a big challenge even for advanced manufacturing sectors. Nickel-based superalloys are widely used in aircraft industry due to their exceptional thermal resistance which allows retaining mechanical properties up to temperature of 700°C [5].

This fact is decisive for the fracture of the severely deformed material occurring in the shearing zone during machining process. Moreover, it results in the generation of high cutting forces and high amount of heat. Under such boundary process conditions also sliding friction at the tool-chip interface seems to be extremely intensive.

The finite element method (FEM) is often used to obtain knowledge about the forces and the temperatures occurring during the cutting process [11],[16]. The FEM simulations of metal cutting employ several phenomenological plasticity laws including mostly Power Law (PL) and Johnson-Cook (JC) models.

Machining simulation practice has documented that the application of the sufficient constitutive model is a predominant condition leading to acceptable predictions.

---

<sup>1</sup> Faculty of Mechanical Engineering, Opole University of Technology, Opole, Poland

<sup>2</sup> PZL WSK Rzeszów, Rzeszów, Poland

\* E-mail: [p.nieslony@po.opole.pl](mailto:p.nieslony@po.opole.pl)

As previously revealed [1],[8],[15] one of the important model parameters is the friction coefficient ( $\mu$ ) but its influence on the FEM simulation of the mechanical and thermal outputs is not yet sufficiently explored.

Own preliminary studies suggest that the role of  $\mu$  depends on the type of the FEM material model used. In addition, the mathematical structure of the model describing the behaviour of the tool/coating-chip is also important in prediction of mechanical and thermal process outputs [3],[4],[15]. It can then be concluded that the influence of friction coefficient on the mechanical and thermal characteristics is not still properly reflected by FE simulation results [1],[2].

The paper is, in general, focused on the influence of the friction coefficient and the constitutive models of the workpiece material on the results and simulation accuracy when performing three (3D) dimensional turning operations of a representative nickel-based alloy-Inconel 718 using TiAlN coated grooved carbide tools.

## 2. METHODOLOGY OF INVESTIGATIONS

In this study, non-orthogonal turning was carried out on a CNC lathe equipped with Kistler9257B piezoelectric dynamometer with 5019B amplifier and NI 6062E, National Instruments, A/D multi-channel board. The visualization of the recorded force signals and their processing was performed using CutPro data acquisition system. The experimental and simulation conditions are specified in Table 1.

Table 1. Configurations of experimental and numerical simulations

Cutting condition	$v_c=80\text{m/min}$ , $a_p=0.125, 0.25, 1.0$ and $2\text{mm}$ , $f=0.1\text{mm/rev}$
Tool data	Grooved tool (KM) type CNMG 120412-UP Sintered carbide insert H10 coated with TiAlN layer of $3\ \mu\text{m}$ thick Cutting edge radius $r_n=50\ \mu\text{m}$
Tool geometry	Cutting tool angles: orthogonal rake $\gamma_0=-5^\circ$ , orthogonal clearance $\alpha_0=5^\circ$ , back rake $\gamma_p=-4.55^\circ$ , side rake $\gamma_f=-5.41^\circ$ , tool inclination angle $\lambda_s=-5.0^\circ$ Tool nose radius $r_\epsilon=1.2\text{mm}$
Constitutive material models	Power Law (PL) Johnson-Cook model with defined thermophysical properties of workpiece material (JC)
Simulation models	Three dimensional (3D)

In these investigations FEM simulations were performed for two fundamental constitutive models including Power Law (PL) and Johnson-Cook (JC) models (set of parameters are shown in Table 2). The mathematical formulations are presented in [9] and [10] respectively.

Table 2. Johnson–Cook (JC) [7],[12],[13],[14] material models parameters for Inconel 718

Code	A, MPa	B, MPa	n	C	m	$\epsilon_0^p$ 1/s
JC	450	1700	0.65	0.017	1.3	1.0
Melting temperature				1260 °C		
Young modulus				200GPa		
Poisson ratio				0.294		
Coefficient of thermal expansion				1.2 10 <sup>-5</sup> 1/K		
Density				8206kg/m <sup>-3</sup>		

The JC model is a well-accepted and numerically robust constitutive material model and highly utilized in modeling and simulation studies. This model assumes that the slope of the flow stress curve is independently affected by strain hardening, strain rate sensitivity and thermal softening behaviors. Relevant parameters in the PL model were selected from the material data base of AdvantEdge FEM package for a Inconel 718 alloy and the ISO P20 carbide substrate along with the deposited TiAlN coating. The thermophysical properties of the titanium-aluminium nitride (TiAlN) were implemented into the constitutive models using an experimental set of data. The changes of the diffusivity  $\alpha$  and specific heat  $c_p$  as a function of temperature are presented in the form of the following equation:

$$c_p(T) = 416 + 0.283 T - 1.016 \cdot 10^{-3} T^2 + 2.581 \cdot 10^{-6} T^3 - 2.246 \cdot 10^{-9} T^4 + 6.307 \cdot 10^{-13} T^5 \quad (1)$$

$$\alpha(T) = 3.08 \cdot 10^{-6} + 3.42 \cdot 10^{-9} T + 8.4 \cdot 10^{-12} T^2 - 3.03 \cdot 10^{-14} T^3 + 2.97 \cdot 10^{-17} T^4 - 9.18 \cdot 10^{-21} T^5 \quad (2)$$

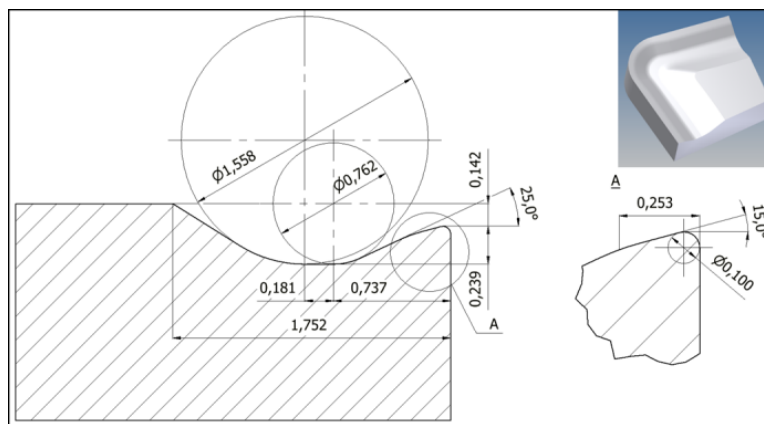


Fig. 1. Dimensioned cross-section of Kennametal cutting insert type CNMG 120412-UP with CAD model of tool edge used in FEM simulation [6]

The experimental study and FEM simulations were performed for grooved rake faces and CNMG 120412-UP cutting tool inserts produced by Kennametal were used [6]. The measured value of the cutting edge radius for this insert coated by TiAlN monolayer was equal to  $r_n=50\mu\text{m}$ . For the FEM simulation the original 3D CAD model of the grooved cutting insert is used. The dimensioned groove and cutting edge along with magnified corner area are presented in Fig. 1.

### 3. EXPERIMENTAL RESULTS

FEM simulations of turning operations of Inconel 718 with coated carbide tools are performed using 3D FEM package. For each of the tested PL and JC constitutive models, a series of simulations for three different values of  $\mu = 0.2, 0.5$  and  $0.8$  were performed. The range of  $\mu$  variation was selected experimentally based on tribo-tests using a pin-on-disc device.

Table 3. Comparison of friction coefficient at different sliding speeds and normal forces

Sliding speed, m/min	Force, N	Friction coefficient	First Quartile	Third Quartile	Max	Min
30	10	0.7	0.67	0.73	1.1	0.43
60	10	0.58	0.53	0.66	0.77	0.36
90	10	1.2	1	1.2	1.3	0.63
30	20	0.61	0.59	0.62	0.65	0.47
60	20	0.56	0.54	0.58	0.62	0.51
90	20	0.7	0.68	0.72	0.75	0.45
30	30	0.54	0.53	0.55	0.56	0.49
60	30	0.56	0.55	0.57	0.59	0.47
90	30	0.5	0.53	0.59	0.78	0.22

During tribo-tests the sliding velocity and the normal load were varied at three levels, i.e.  $v_s=30, 60$  i  $90\text{m/min}$  and  $F_n=10, 20$  i  $30\text{N}$ . The results of tribo-tests are presented in the form of so-called Box-Whisker Plots as in Fig. 2 and selected in Table 3. It was observed that for a lower normal load the predicted  $\mu$  values are distinctly higher than for other loads exerted, independently of the sliding velocity used. Apart from the test with the lowest load ( $v_s = 90\text{m/min}, F_n=10\text{N}$ ) the predicted  $\mu$  values vary in the range of  $0.5 - 0.8$ .

The literature survey [2],[8],[16] indicates that FEM simulations of turning operations are done with constant Coulomb friction of  $0.5$ . In contrast, in this study the changes of  $\mu$  were extended to the upper and lower boundaries of  $0.8$  and  $0.2$  as show in Fig. 2. As a result, the sensitivity of the two constitutive models to the variable friction was checked including mechanical and thermal outputs. It should be noted in Fig. 2 that the upper range of  $\mu$  above  $0.5$  was selected based on the results of tribo-testing by means of a pin-on-disc device.

FEM predictions of the component forces for the PL and JC constitutive laws and the selected values of the friction coefficient are compared with the measured forces in Fig. 3. It can then be, in general, reasoned that for both FEM models the predicted values of the cutting force are higher in comparison to the measured values. This fact is visualized in Fig. 3a. On the other hand, Fig. 3b and 3c document that the measured values of the feed  $F_f$  and passive  $F_p$  forces are in the range of FEM predictions using PL and JC laws. It should be noticed that similar trends were obtained in FEM simulations of turning operations of a Ti6Al4V alloy. In particular, the trend that the force values increase with the increase of the depth of cut ( $a_p$ ) is well observed. The general conclusion resulting from a set of graphs presenting force vs. depth of cut is that the friction coefficient influences the FEM force predictions. A more detailed percentage comparison is carried out in Fig. 6.

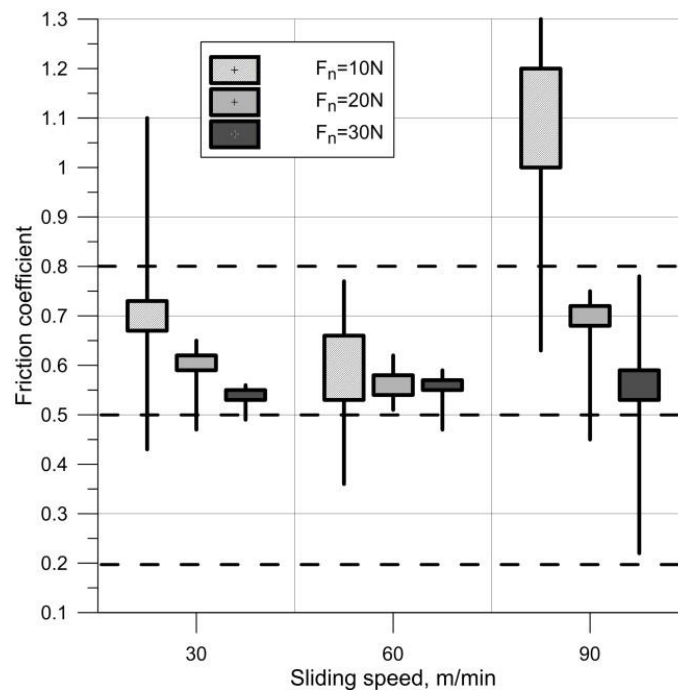


Fig. 2. Values of  $\mu$  obtained from tribo-tests for variable sliding velocity  $v_s$  and normal load  $F_n$ . Experimental results are presented in the form of the median and quartiles with the maximum values

The influence of the friction coefficient on average values of the predicted cutting temperature for the two constitutive models used is presented in Fig. 4.

As can be seen there the increase of the depth of cut causes that the cutting temperature increases, in general, for both constitutive models applied. However, higher values of the cutting temperature were obtained for the JC model. In both cases the thermophysical properties ( $c_p$ ,  $\alpha$ ) of Inconel 718 were defined as temperature-dependent according to Eqns. (1) and (2). Substantial differences in the predicted temperatures were revealed for these constitutive models. As can also be noted the trend in the relationship  $\mu$  vs.  $T$  is that the average cutting temperature increases with the increase of the friction coefficient from 0.2 to 0.8.

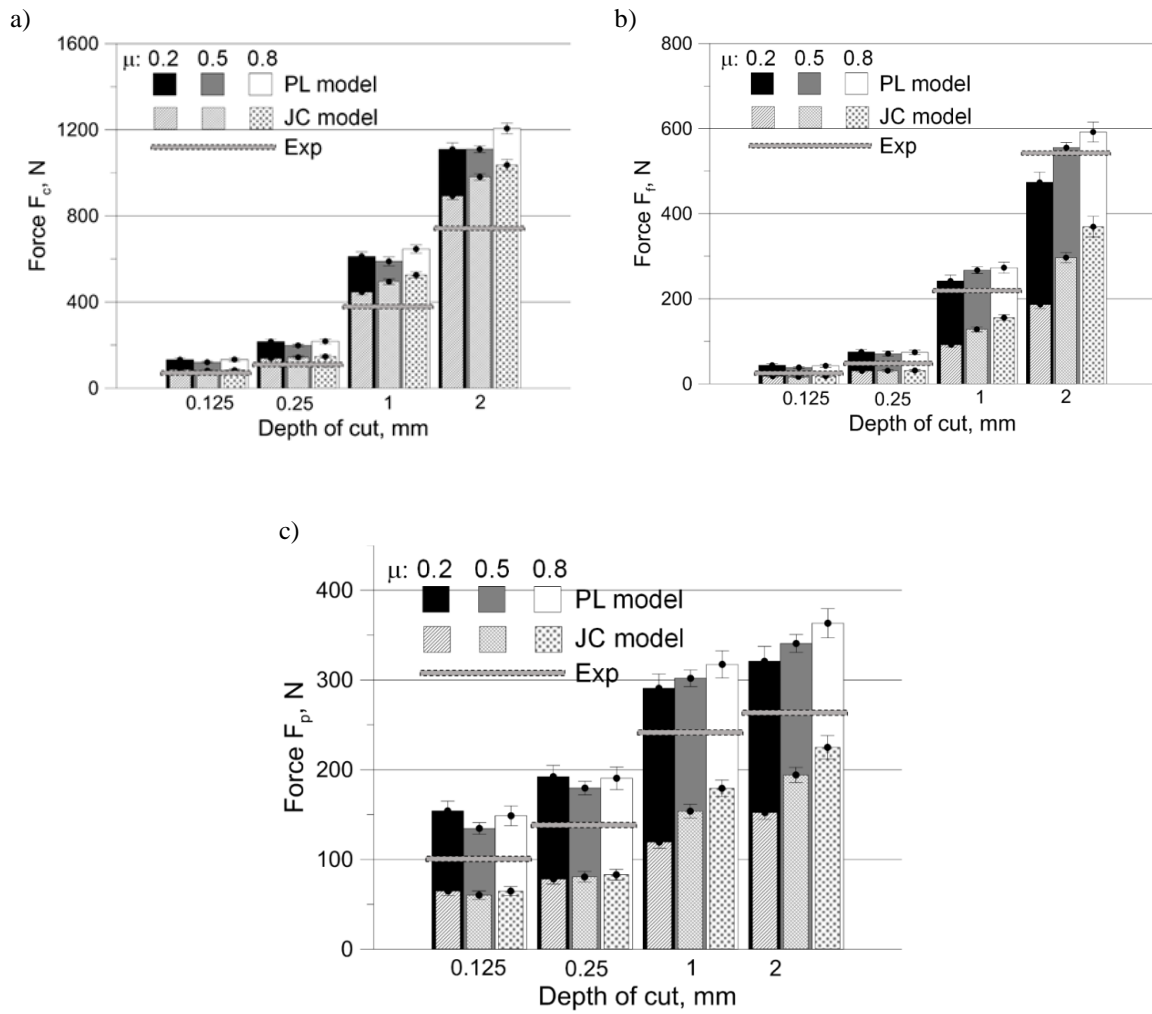


Fig. 3. Values of cutting (a), feed (b) and passive (c) forces predicted from PL and JC constitutive models for variable  $\mu$  vs. experimental results

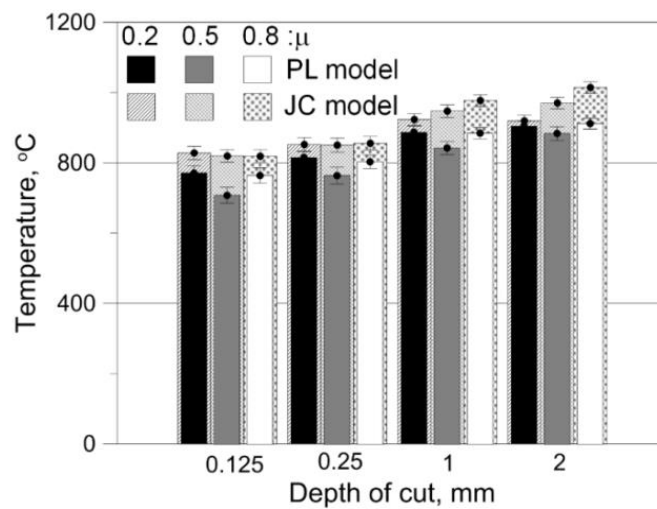


Fig. 4. Average cutting temperature obtained for FEM simulations using PL and JC models for variable friction coefficient

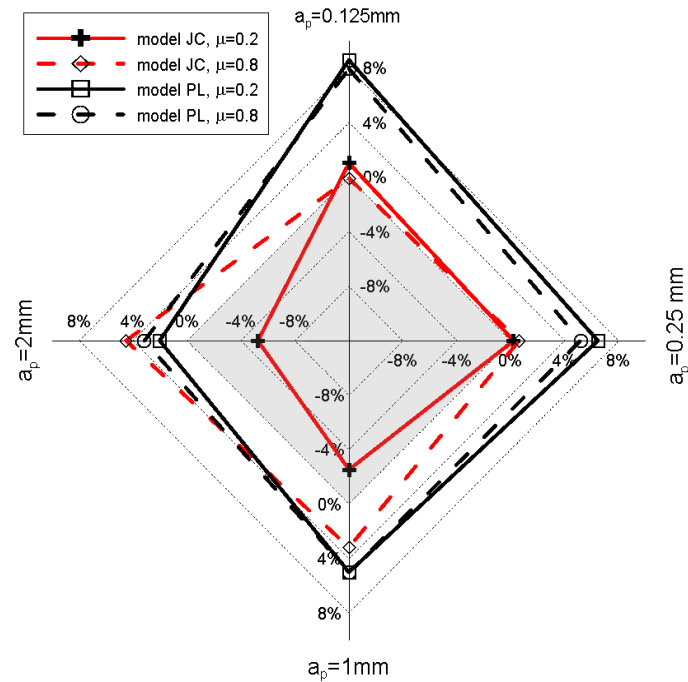


Fig. 5. Radar plot showing percentage differences of cutting temperatures obtained for PL and JC models for variable friction coefficient in comparison to FEM prediction with constant  $\mu = 0.5$

The sensitivity of FEM simulations to the variations of  $\mu$  was established based on the temperature differences in comparison to the reference temperature predicted for  $\mu = 0.5$ . Relevant radar graph is shown in Fig. 5.

As can be seen in Fig. 5 for the JC model, the differences are equal to  $+4\%$  and  $-4\%$  for  $\mu = 0.8$  and  $0.2$  respectively. Taking into account that the friction coefficient is correlated with the friction energy dissipated in the cutting zone, the increase of  $\mu$  should result in the increase of the friction energy. Based on Fig. 4, this effect was not clearly observed for lower depths of cut of  $0.125\text{mm}$  and  $0.25\text{mm}$ .

On the other hand, different effects were observed for the PL model. In this case, the highest temperatures were predicted for the lowest  $\mu = 0.2$  and, oppositely, the lowest cutting temperatures correspond to the highest  $\mu = 0.5$ . In addition, for the reference  $\mu = 0.5$  the cutting temperature increases by  $4\%$  and  $8\%$  for the depth of cut of  $0.125\text{mm}$  and  $0.25\text{mm}$  respectively (Fig. 5). It is interesting to note that the maximum temperature difference was obtained for small depths of cut for which the temperature differences were very low when using the JC model.

When considering mechanical aspects, it can be noted that for lower depths of cut of  $0.125\text{mm}$  and  $0.25\text{mm}$  the values of force components  $F_c$ ,  $F_f$  and  $F_p$  were higher for the lowest  $\mu = 0.2$ . Consequently, the higher cutting force implicates the higher cutting energy and as a result, higher cutting temperature.

Practically, the same effect was obtained for higher depths of cut of  $a_p=1$  and  $2\text{mm}$ . Only for  $\mu = 0.2$  the values of the cutting force  $F_c$  are higher by about  $100\%$  than for lower depths of cut and other values of  $\mu$ .

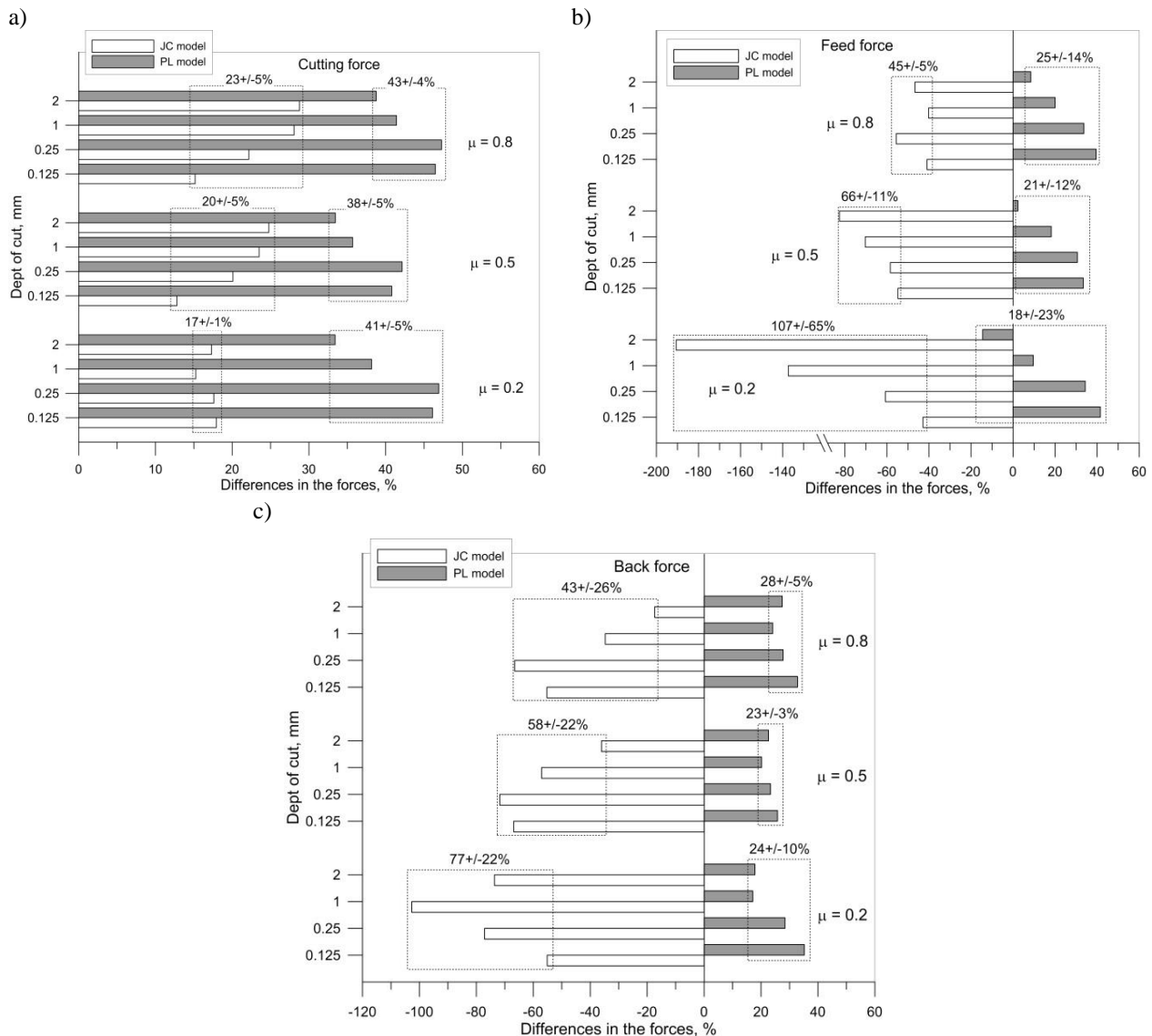


Fig. 6. Percentage differences in component forces: cutting (a) feed (b) and passive (c) in comparison to experimental data

The influence of friction conditions defined for FEM simulations on the changes of three component forces can be easily assessed based on bar diagrams shown in Fig. 6. These diagrams illustrate the percentage differences of  $F_c$ ,  $F_f$  and  $F_p$  values in comparison to experimental results.

The first important fact is that the predicted values of the cutting force  $F_c$  overestimate the measured results for all values of the depth of cut and all selected values of  $\mu$ . Minimum differences in the range of 17 – 23% were obtained for  $\mu$  equal to 0.2 and 0.8 and the JC material model. However, these differences were distinctly higher and in the order of 38-43%.

The influence of  $\mu$  related to a variable depth of cut was small enough and equal to  $(\pm 1\%) - (\pm 5\%)$  and about  $\pm 5\%$  for the JC and PL models respectively.



The best statistical fitting was documented for FEM simulations of the  $F_c$  force using the JC model in the case of finish turning with lower depth of cuts. Similarly, the minimum difference of about  $17\% \pm 1\%$  was when friction coefficient  $\mu=0.2$ .

Quite different influence of the constitutive model was revealed for the  $F_f$  and  $F_p$  forces. The predicted force values were underestimated for the JC model and overestimated for the PL model. In the case of PL model the overestimation ranges from 18% to 28% as show In Fig. 6b and c.

The underestimation corresponding to the JC model was distinctly higher and ranges from 45% to 107%. In particular, such a high disagreement between predicted and measured force values were recorded for the JC model, the minimum value of  $\mu = 0.2$  and the depths of cut of  $a_p=1$  and 2mm characteristic for rough turning. It is rather evident that for the JC model simulation improvement is not possible for a lower friction.

On the other hand, much better simulation results were obtained for the PL material model. The overestimation of measured  $F_f$  and  $F_p$  forces is in the range of that obtained for the  $F_c$  force and the JC model. In addition, the simulation algorithm is more sensitive to changes of the depth of cut. The best fitting was obtained for prediction of the feed force  $F_f$  and  $a_p=1$ mm and 2mm. Under such machining conditions, the overestimation level is 10% (exceptionally 20%) as shown in Fig. 6b.

The chip shapes and Mises stress distribution in the cutting zone determined for different constitutive material models (PL and JC) and a variable friction coefficient are presented in Fig. 7. It has been found, based on the visual observations that only the constitutive material models influence the chip formation.

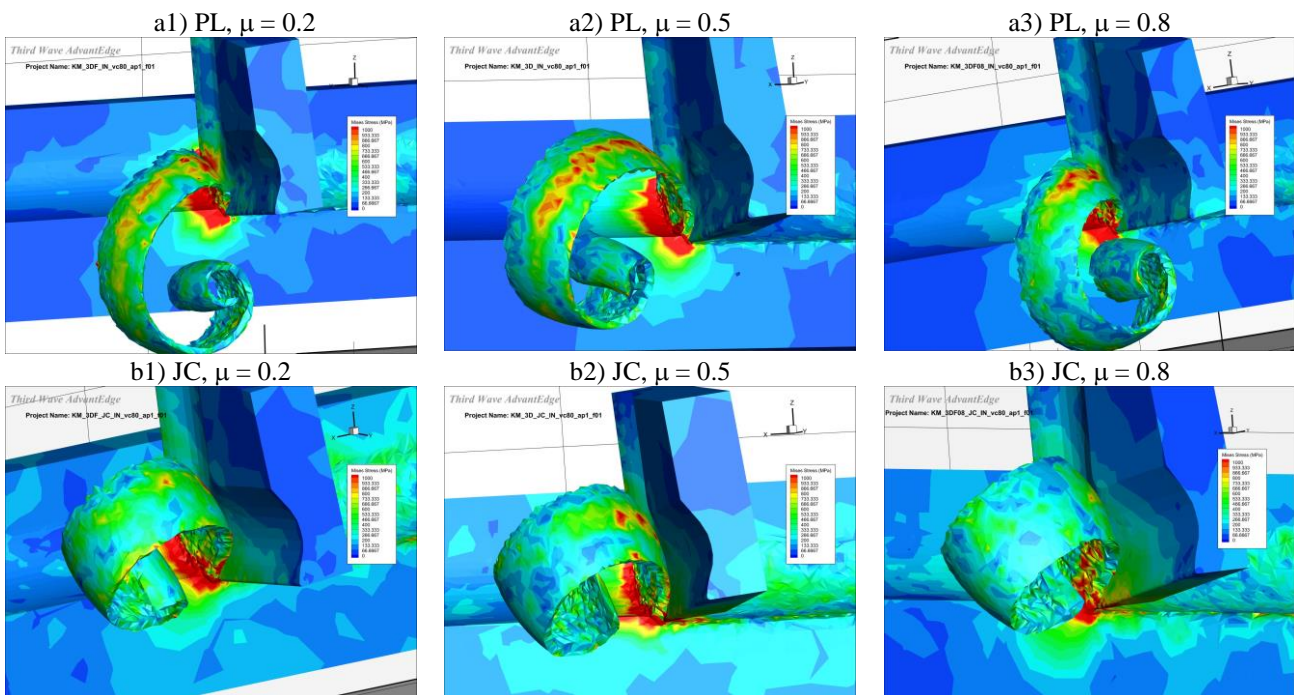


Fig. 7. Chip shapes and Mises stress maps created by 3D FEM simulations using different constitutive material models (PL and JC) and friction coefficients. Process parameters:  $a_p=1.0$ mm, cutting distance  $l_c=20$ mm

The PL model results in a more curly chip. It was also observed that the chips are longer for the PL model. This may result from the different chip thicknesses obtained for PL and JC models. In order to keep the constant chip volume, longer chips should correspond with the smaller thickness. The analysis of the chip shape and Mises stress distribution was done for 3D simulation using a slice technique illustrated in Fig. 9. The cross-sectional plane was created axially through the chip and perpendicular to the ZY plane as show in Fig. 8.

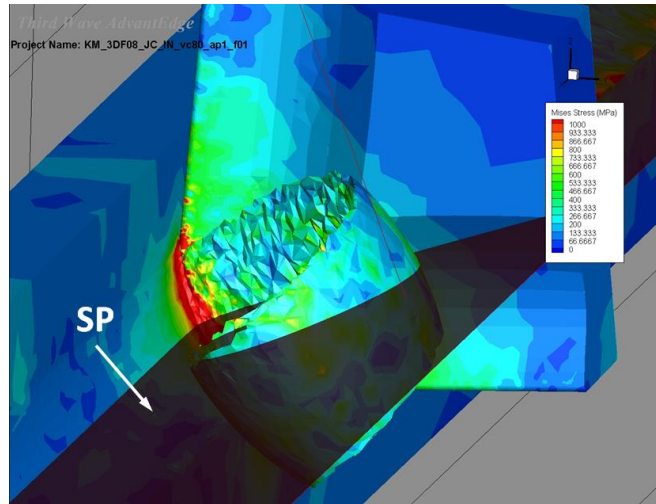


Fig. 8. Localization of the slice plane SP in 3D FEM simulation area

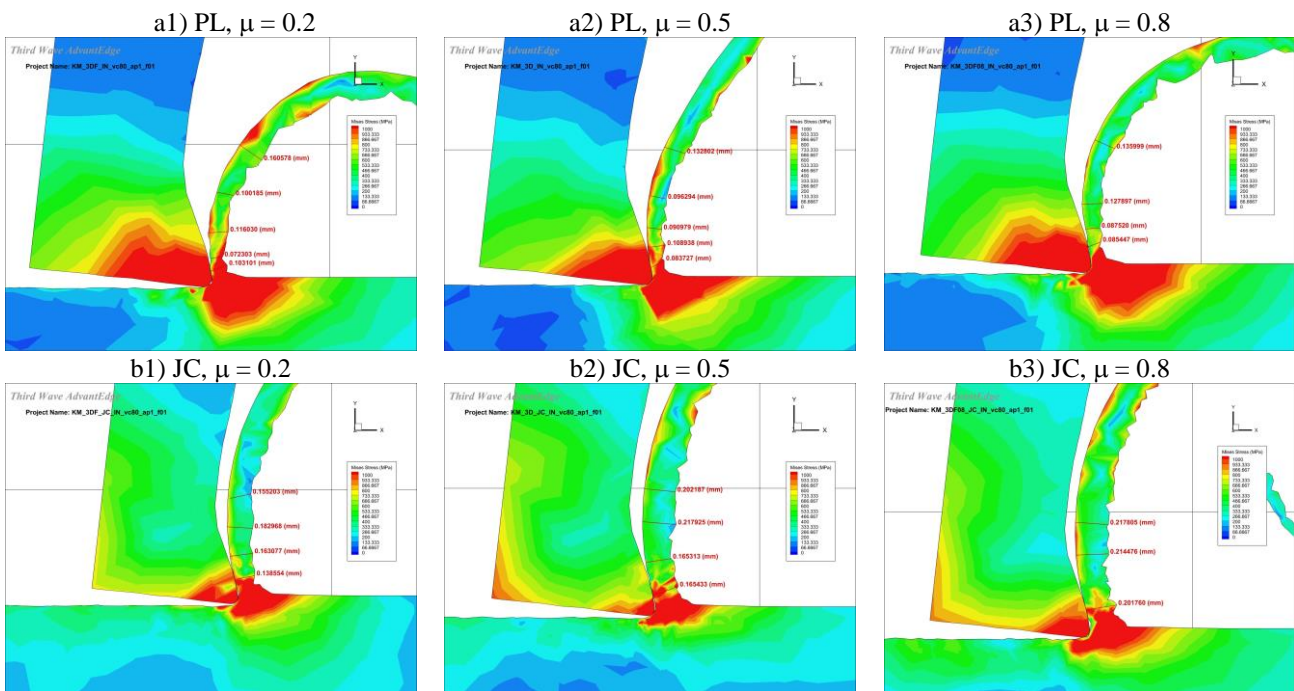


Fig. 9. Chip configurations and Mises stress maps obtained for different constitutive material models (PL and JC) and values of friction coefficient. Process parameters:  $a_p=1.0\text{mm}$ , cutting distance  $l_c=20\text{mm}$

As shown in Figs. 9a1-a3 the average chip thickness obtained by the PL model does not change and is equal to about 0.10-0.11mm. In contrast, it changes from 0.16 to 0.21mm when the JC model is applied. It should then be noted in Fig. 9 that thicker chips presented in Fig.7 are produced with higher chip curvature (chips are visibly longer, as for example case # a1 vs. case # b1).

#### 4. CONCLUSIONS

Based on the experimental results and FEM predictions the conclusions are as follows:

- Tribological tests support the selection of  $\mu$  values for FEM simulations. As a result, three values of  $\mu$  equal to 0.2, 0.5 and 0.8 were selected.
- The resolution of the resultant cutting force was different for the two constitutive models (JC and PL) applied.
- The FEM predicted values of the cutting force  $F_c$  overestimate the experimental values. In relation to other component forces  $F_f$  and  $F_p$ , simulations with PL model lead to overestimation, whereas simulations with JC model result in underestimation of the measured forces.
- The best statistical fitting was obtained when the cutting force  $F_c$  was simulated using JC model. For other component forces the most suitable was the PL model PL.
- The effect of friction coefficient on the cutting forces was observed but the sensitivity of the constitutive models was different. In general, the effect of  $\mu$  on cutting forces is more visible for the JC model. On the other hand, changes of  $F_c$  force and cutting temperature are marginal and difficult for simple physical interpretation.
- The dependence of average values of the cutting temperature on the friction coefficient was determined for the JC model only.
- The general conclusion is that for FEM based machining simulations of Inconel 718 the JC model should be applied instead the PL model proposed in AdvantEdge FEM package. However, further improvements of the model parameters are needed.

#### ACKNOWLEDGEMENTS

*This investigation has been carried out as a part of the research project No. PBS1-178595 funded by the Polish National Center for Research and Development (NCBiR).*

#### REFERENCES

- [1] BANERJEE N., SHARMA A., 2014, *Identification of a friction model for minimum quantity lubrication machining*, J. Clean. Product, 83, 437–443.
- [2] DEVILLEZ A., SCHNEIDER F., DOMINIAK S., DUDZINSKI D., LARROUQUERE D., 2007, *Cutting forces and wear in dry machining of Inconel 718 with coated carbide tools*, Wear. 262, 931–942.

- [3] EGAÑA A., RECH J., ARRAZOLA P.J., 2012, *Characterization of friction coefficient and heat partition coefficient during machining of a TiAl6V4 titanium alloy and a cemented carbide*, Tribol. Trans., 55, 665–676.
- [4] GRZESIK W., NIESŁONY P., 2004, *Prediction of friction and heat flow in machining incorporating thermophysical properties of the coating–chip interface*, Wear, 256, 108–177.
- [5] JEMIELNIAK K., 2009, *Rough turning of Inconel 718*, Adv. Manuf. Sci. Technol., 33/3, 5–15.
- [6] KENNAMETAL 2013, May 15. Available: <http://www.kennametal.com>.
- [7] Material Properties Database, MPDB v. 7.51, 2013, JAHM Software, Inc.
- [8] MITROFANOV A.V., BABITSKY V.I., SILBERSCHMIDT V.V., 2004, *Finite element analysis of ultrasonically assisted turning of Inconel 718*, J. Mat. Proc. Technol., 153–154, 233–239.
- [9] NIESŁONY P., GRZESIK W., CHUDY R., LASKOWSKI P., HABRAT W., 2013, *3D FEM simulation of titanium machining*, International Conference on Advanced Manufacturing Engineering and Technologies - NEWTECH 2013, 31–40.
- [10] NIESŁONY P., GRZESIK W., LASKOWSKI P., HABRAT W., 2013, *FEM-based modelling of the influence of thermophysical properties of work and cutting tool materials on the process performance*. Procedia CIRP 8, 3-8.
- [11] SOO S.L., ASPINWALL D.K., DEWES R.C., 2004, *3D FE modelling of the cutting of Inconel 718*, J. Mat. Proc. Technol., 150, 116–123.
- [12] UHLMANN E., GERSTENBERGER R., KUHNERT J., 2013, *Cutting simulation with the meshfree Finite Pointset Method*, 14th CIRP Conference on Modeling of Machining Operations, Procedia CIRP, 391–396.
- [13] UHLMANN E., GRAF VON DER SCHULENBURG M., ZETTIER R., 2007, *Finite Element Modeling and cutting simulation of Inconel 718*,. CIRP Annals - Manufacturing Technology, 56/1, 61–64.
- [14] YOO J.T., YOON J.H., LEE H.S., YOUN S.K., 2012, *Material characterization of Inconel 718 from free bulging test at high temperature*, J. Mech. Sci. Technol., 26, 2101–2105.
- [15] ZEMZEMI F., RECH J., BEN SALEM W., DOGUI A., KAPSA Ph., 2014, *Identification of friction and heat partition model at the tool-chip-workpiece interfaces in dry cutting of an Inconel 718 alloy with CBN and coated carbide tools*, Adv. Manuf. Sci. Technol., 38/1, 5–22.
- [16] ZHEN C.Y., DING H.Z., XIN C.H., CHANG F.Y., YONG S.L., YING M., 2010, *The simulation of cutting force and temperature field in turning of Inconel 718*, Key Eng. Mat. 458, 149–154.